STEM CELLS AND DEVELOPMENT
Volume 20, Number 6, 2011

DOI: 10.1089/scd.2010.0379

Amniotic Mesenchymal Stem Cells Enhance Normal Fetal Wound Healing

Justin D. Klein,[1] Christopher G.B. Turner,[1] Shaun A. Steigman,[1] Azra Ahmed,[1] David Zurakowski,[1] Elof Eriksson,[2] and Dario O. Fauza[1]

Fetal wound healing involves minimal inflammation and limited scarring. Its mechanisms, which remain to be fully elucidated, hold valuable clues for wound healing modulation and the development of regenerative strategies. We sought to determine whether fetal wound healing includes a hitherto unrecognized cellular component. Two sets of fetal lambs underwent consecutive experiments at midgestation. First, fetuses received an intra-amniotic infusion of labeled autologous amniotic mesenchymal stem cells (aMSCs), in parallel to different surgical manipulations. Subsequently, fetuses underwent creation of 2 symmetrical, size-matched skin wounds, both encased by a titanium chamber. One of the chambers was left open and the other covered with a semipermeable membrane that allowed for passage of water and all molecules, but not any cells. Survivors from both experiments had their wounds analyzed at different time points before term. Labeled aMSCs were documented in all concurrent surgical wounds. Covered wounds showed a significantly slower healing rate than open wounds. Paired comparisons indicated significantly lower elastin levels in covered wounds at the mid time points, with no significant differences in collagen levels. No significant changes in hyaluronic acid levels were detected between the wound types. Immunohistochemistry for substance P was positive in both open and covered wounds. We conclude that fetal wound healing encompasses an autologous yet exogenous cellular component in naturally occurring aMSCs. Although seemingly not absolutely essential to the healing process, amniotic cells expedite wound closure and enhance its extracellular matrix profile. Further scrutiny into translational implications of this finding is warranted.

Introduction

Within the spectrum of reparative and regenerative processes, fetal wound healing is closer to the latter than to the former. When compared with healing at any stage of postnatal life, wound healing in the fetus involves significantly less inflammation and can be almost scarless, particularly early in gestation. The mechanisms behind the fetus' greatly enhanced capacity to heal wounds remain poorly understood [1]. Yet, there lay clues as to means to enhance wound healing postnatally, with far reaching therapeutic implications, well beyond purely tegumental repair. To date, the focus of fetal wound healing research has been on the peculiarities of local molecular pathways and gene expression patterns, for example, the widely described upregulation of hyaluronan, a major extracellular matrix component of the epidermis that controls keratinocyte proliferation and differentiation [2,3].

In this study, we sought to determine whether there is a hitherto unnoticed cellular component to fetal wound healing. Throughout gestation, the amniotic fluid harbors a unique population of fetal mesenchymal stem cells [4–6]. Mesenchymal stem cells from other sources, for instance, bone marrow, are known to home in to injured sites and help promote local repair in postnatal life [7–9]. We hypothesized that amniotic mesenchymal stem cells (aMSCs) participate in fetal wound healing.

To test this hypothesis, we chose to develop 2 ovine surgical models, due to sheep's well known tolerance to prenatal surgical interventions without ensuing preterm labor, as well as its reasonably long gestation time (term = 145 days), which allows for meaningful cell processing in between the >1 surgical procedure required in part of our experimental design.

Materials and Methods

This study was approved by the Institutional Animal Care and Use Committee of Children's Hospital Boston under protocol number 08-10-1224. Two sets of fetal lambs were

[1]Department of Surgery, Children's Hospital Boston and Harvard Medical School, Boston, Massachusetts.
[2]Department of Plastic Surgery, Brigham & Women's Hospital and Harvard Medical School, Boston, Massachusetts.

submitted to 2 independent and consecutive experiments, as follows:

Experiment I

Amniotic fluid procurement and fetal procedure # 1. Time-dated pregnant ewes at 88.3 ± 2.8 days of gestation were anesthetized with 2%–4% isoflurane (Baxter Healthcare, Deerfield, IL). Animals received 20 mg/kg of cefazolin (Sandoz, Princeton, NJ) intravenously within 1 h before surgery. Through a median longitudinal laparotomy, we exposed the bicornuate uterus. After hysterotomy, fetal lambs ($n = 12$) underwent procurement of 50 mL of amniotic fluid for processing (details below), followed by a left lateral thoracotomy, which was closed in layers. The fetuses were repositioned back into the amniotic cavity, into which 500 mg of cefazolin (Sandoz) was infused and the hysterotomy was closed in 1 single layer together with the gestational membranes with a reusable TA 90-mm Titanium surgical stapler (US Surgical, Norwalk, CT). The mother's abdomen was closed in layers. The ewes received 20,000 U/kg of penicillin-Gg (Vetco, St. Joseph, MO) intramuscularly daily for the first 3 postoperative days (POD); otherwise gestation was allowed to progress normally.

aMSC processing. A population of mesenchymal stem cells was isolated from the amniotic samples as we have previously described [10]. Their mesenchymal progenitor phenotype was characterized by multicolor flow cytometry with unconjugated, mouse monoclonal antibodies previously validated for use in sheep [11,12]. The antibodies used were CD29 (dilution 1:10; VMRD, Pullman, WA), CD31/PECAM-1 (dilution 1:2; Serotec, Oxford, United Kingdom), CD44 (Serotec), CD90/Thy-1 (dilution 1:10; BD Biosciences, Bedford, MA), and CD105/SH2/endoglin (dilution 1:10; BD Biosciences). After several washes in 0.1% bovine serum albumin (Sigma-Aldrich, St. Louis, MO), the cells were put on ice for an additional 20 min with a fluorescein isothiocynate-conjugated rabbit anti-mouse immunoglobulin (1:100 dilution, STAR9B; Serotec). Nonspecific cell staining was excluded using a mouse isotype immunoglobulin control. Between 5,000 and 10,000 labeled cells were acquired and analyzed using the Vantage SE cell sorter (BD Biosciences).

To functionally confirm their multipotent differential potential, subsets of the isolated cells from all animals also underwent culture under osteogenic and adipogenic conditions, as follows [13]. For osteogenic differentiation, cells at passage 8 were plated at a density of 5×10^4 cells/cm^2 in 6-well plates containing Dulbecco's modified Eagle's medium, 5% fetal bovine serum, 10,000 U/mL penicillin G sodium, 10 mg/mL streptomycin sulfate, 5 mM β-glycerophosphate, 50 μM ascorbic acid-2 phosphate, and 100 nM dexamethasone (all from Sigma-Aldrich). As negative controls, cells were cultured in parallel in the standard culture medium. After 21 days, osteogenic differentiation was assessed according to a modified von Kossa staining protocol [14]. Briefly, the cells were fixed in 4% paraformaldehyde for 10 min and stained with 2% silver nitrate (Fisher Scientific, Fairlawn, NJ) for 30 min under ultraviolet light. After 3 washes in distilled water, the cells were placed in 2.5% sodium thiosulfate (Sigma-Aldrich) for 5 min, washed once more in distilled water, and assessed qualitatively for silver-stained mineralization under an inverted microscope. For adipogenic differentiation, cells at passage 8 were plated at a density of $3–5 \times 10^4$ cells/cm^2 in 6-well plates containing Dulbecco's modified Eagle's medium, 10% fetal bovine serum, 10,000 U/mL penicillin G sodium, 10 mg/mL streptomycin sulfate, 60 μM indomethacin, 1 μM dexamethasone, 10 μg/mL insulin, and 0.5 mM 3-isobutyl-1-methylxanthine (all from Sigma-Aldrich). As negative controls, cells were cultured in parallel in the standard medium. After 21 days, cells were fixed in 10% formalin and stained with 0.5% Oil-O-Red (Sigma-Aldrich) in 60% isopropanol (Fisher) for 10 min. The cells were washed with distilled water and assessed qualitatively for the presence of orange-red intracellular lipid vacuoles under an inverted microscope.

Isolated aMSCs were labeled with green fluorescent protein (GFP) by retroviral infection based on methods previously described [15]. Briefly, amphotropic viruses were prepared by cotransfecting the construct, pMIG, with a pCL-10A1 plasmid (Imgenex, San Diego, CA) into human embryonic kidney 293 cells (Q-Biogene, Montreal, Canada) using the FuGENE 6 (Roche Applied Science, Indianapolis, IN), or the Lipofectamine 2000 (Invitrogen, Carlsbad, CA) transfection reagents. Supernatants were collected at 48 and 72 h post-transfection, filtered, and used to infect the mesenchymal amniocytes. Virus-containing medium was removed after a minimum of 4 h (if FuGENE 6 was used), or 12 h (if Lipofectamine 2000 was used), when the fresh culture medium was added. Labeling was confirmed and quantified by fluorescence-activated cell sorting analysis using a MoFlo cytometer (Cytomation, Fort Collins, CO) [15].

Labeled aMSC delivery and fetal procedure # 2. Survivors from the first operation ($n = 11$) underwent a second procedure at 123.4 ± 2.3 days' gestation, when a 2 cm longitudinal midline cervicotomy closed in layers was performed. At that time, a subset of animals also underwent concomitant transverse subtotal ear resections ($n = 8$ wounds), with the resulting exposed cartilage being left to heal by secondary intention. After the fetal manipulations the amniotic cavity was instilled with $3.22 \pm 4.32 \times 10^9$ (1.4×10^6–1.5×10^{10}) of the expanded autologous aMSCs, with a $30.26\% \pm 20.29\%$ (12.9%–62.4%) degree of GFP transfection. This relatively low transfection rate was expected given the somewhat short time in between the 2 fetal surgeries. The amniotic cavity was infused with 500 mg of cefazolin (Sandoz) and the hysterotomy was closed in one single layer together with the gestational membranes with a reusable TA 90-mm Titanium surgical stapler (US Surgical). The mother's abdomen was closed in layers. The ewes received 20,000 U/kg of penicillin-Gg (Vetco) intramuscularly daily for the first 3 POD; otherwise gestation was allowed to continue normally.

Wound analyses. Survivors of the second fetal surgery ($n = 10$) were euthanized 7–14 days thereafter, before the end of gestation, when all their wounds were analyzed. Standard histomorphologic evaluations were in paraffin-embedded specimens sectioned and stained with hematoxylin and eosin. Due to significant autofluorescence in control specimens, labeled cells were detected by immunohistochemistry for GFP performed on fixed specimens using a murine monoclonal anti-GFP antibody (JL-8; Clontech, Mountain View, CA) at 1:200 dilution, including exclusion of nonspecific cell staining with a mouse isotype immunoglobulin control, as detailed elsewhere [16]. Secondary detection was performed with the ultraView Universal DAB detection kit (Ventana, Tucson, AZ), per manufacturer's instructions. All histological examinations of fixed specimens were performed under a light microscope (Carl Zeiss, Jena, Germany) specially

equipped for use with a digital camera (Canon Powershot S3 IS; Canon USA, Lake Success, NY).

Experiment II

To determine whether an eventual presence of aMSCs in fetal wounds, as investigated in experiment I, could not be simply an epiphenomenon, we selectively deprived a subset of fetal wounds from exposure to amniotic cells, but not to any molecule dissolved in amniotic fluid, as follows.

Selective fetal wound exposure. Time-dated pregnant ewes at 102.1 ± 3.1 days of gestation were anesthetized with 2%–4% isoflurane (Baxter Healthcare). Animals received 20 mg/kg of cefazolin (Sandoz) intravenously within 1 h before surgery. Through a median longitudinal laparotomy, we exposed the bicornuate uterus. After hysterotomy, fetal lambs ($n = 17$) underwent creation of 2 symmetrical, size-matched (1 cm^2), full-thickness dermal wounds ($n = 34$) on the proximal aspects of both hind limbs. Attention was taken so as not to use electrocautery at any time. Each wound was hermetically encased laterally by a custom-made titanium chamber [17]. On each fetus, one of the chambers was left open so that the wound was fully exposed to the amniotic cavity (control wound) and the other was closed with a semipermeable, hydrophilic polyvinylidene fluoride membrane with 0.65 μm pores (DVPP04700; Millipore, Carrigtwohill, Ireland), which allowed for passage of water and all molecules, but not any cells (covered wound; Fig. 1). The fetuses were then repositioned back into the amniotic cavity and the hysterotomy was closed in one single layer together with the gestational membranes with a reusable TA 90-mm Titanium surgical stapler (US Surgical). The maternal abdomen was closed in layers. The ewes received 20,000 U/kg of penicillin-Gg (Vetco) intramuscularly daily for the first 3 POD; otherwise, gestation was allowed to progress normally.

Wound analyses. Survivors ($n = 10$) had their wounds ($n = 20$) submitted to multiple analyses at different time points, namely, 5/6, 9, 14, 20, and 32 days postoperatively (2 animals/4 wounds per time point), before term. After removal of the titanium chambers, gross photographs were taken with a digital camera (Canon Powershot S3 IS) at a constant depth of field. Absolute area measurements of the residual open wounds were performed on the photographs using an image analysis freeware (ImageJ, http://rsbweb.nih.gov/ij/) [18].

Histomorphologic evaluations were performed in paraffin-embedded specimens, sectioned and stained with hematoxylin and eosin, Masson's trichrome, and Van Gieson's. Representative sections also underwent immunohistochemical staining for type-III collagen (YMCAF-5850; Accurate Chemical & Scientific Corp., Westbury, NY) and for Substance P (Abcam, Cambridge, MA). The latter required a horseradish peroxidase secondary antibody for observation (Abcam). Examination of all fixed specimens was performed under a light microscope (Carl Zeiss) specially equipped for use with a digital camera (Canon Powershot S3 IS).

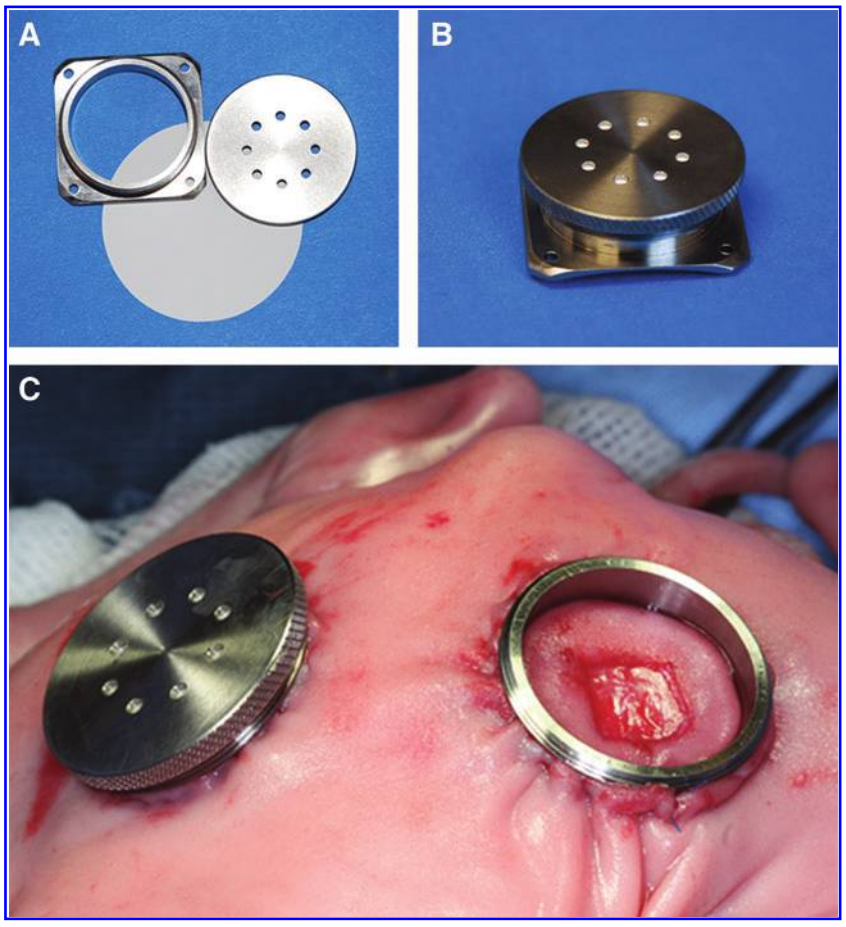

FIG. 1. (A) A titanium chamber and semipermeable hydrophilic membrane, before final assembly. **(B)** An assembled titanium chamber fitted with a semipermeable hydrophilic membrane. **(C)** Both titanium chambers already anchored to 2 symmetrical fetal wounds, one left open (control) and the other covered with a semipermeable membrane as shown in **(A, B)**. Color images available online at www.liebertonline.com/scd

Wound levels of pepsin-soluble collagen (predominantly type-II) and α-elastin were quantified spectrophotometrically using standard protocols as described in previous work [19]. Briefly, representative wound specimens were minced and weighed. Quantification of pepsin-soluble collagen was carried out by digesting each sample with a 1:10 ratio of pepsin (Fisher) to substrate in 0.5 M acetic acid (Fisher) on an orbital shaker at 4°C for 24 h. The collagen content was measured spectrophotometrically at 540 nm (BMG Labtech, Offenburg, Germany) using a Sircol dye reagent and the Sircol assay kit (Biocolor, Belfast, United Kingdom) containing Sirius red according to the manufacturer's instructions. On subsequent samples, α-elastin was extracted by adding 20 volumes of 0.25 M oxalic acid (Sigma-Aldrich) and heating in a boiling water bath for 1 h. This was repeated 4 times, after which the elastin content of the extracts was measured spectrophotometrically at 513 nm (BMG Labtech) using a tetraphenylporphine tetrasulfonate and the Fastin assay kit (Biocolor) according to the manufacturer's instructions.

Lastly, hyaluronan was determined spectroscopically at 405 nm (BMG Labtech) using a commercially available enzyme-linked immunosorbent assay kit (Echelon Biosciences, Salt Lake City, UT) based on a competitive enzyme-linked immunosorbent assay where the colorimetric signal is inversely proportional to the amount of hyaluronan present in the sample [20]. Tissue extraction of hyaluronan was carried out according to manufacturer's instructions. Briefly, after weighing, tissues were minced and digested for 16 h at 60°C with 1 mg/mL papain (Sigma-Aldrich) in 0.2 M acetate buffer (Sigma-Aldrich) containing 10 mM disodium ethylenediaminetetraacetic acid (Sigma-Aldrich) and 10 mM cysteine (Sigma-Aldrich). The reaction was stopped by boiling the samples for 30 min to inactivate the enzyme and the hyaluronan mass of the supernatant was then measured spectroscopically.

Statistical analysis. Two-way repeated-measures analysis of variance was used to compare wound area and extracellular matrix results between covered and open wounds and accounted for the multiple post-hoc paired comparisons at the different time points. The 2-way interaction *F*-test (ie, slope test) was used to assess whether covered and open wounds differed in changes in wound area and extracellular matrix variables over the 32-day time course [21]. Two-tailed values of $P < 0.05$ were considered statistically significant. Statistical analysis was performed using the general linear models procedure in the SPSS software package (version 17.0; SPSS Inc./IBM, Chicago, IL).

Results

Experiment I

Isolated mesenchymal amniocytes showed consistent forward and side scatter profiles across all samples on fluorescence-activated cell sorting analyses and an immunophenotype compatible with that of a mesenchymal stem/progenitor lineage (Fig. 2). Greater than 90% of cells were strongly positive for CD29 and CD44, and 40%–50% of cells showed expression of CD90/Thy-1 and CD105/SH2/endoglin. CD31/PECAM-1 was not detected in any sample, pointing to the absence of endothelial cells in our cultures.

All cells cultured under osteogenic conditions displayed osteogenic differentiation, as confirmed by von Kossa staining, along with evidence of dark calcium aggregates. In like manner, adipogenic differentiation was confirmed in all cells cultured in adipogenic media, as demonstrated by the presence of lipid-rich vacuoles on Oil-O-Red staining. Osteogenic and adipogenic differentiation were not observed in aMSCs grown for 21 days in standard medium.

Labeled aMSCs were documented on monoclonal anti-GFP immunohistochemistry in all cervical and thoracic wounds, although seemingly at a lower density in the thoracotomies (Fig. 3). The fact that there was variable and unquantifiable degrees of dilution of the labeled cells with the native, unprocessed aMSCs prevented cell density measurements in situ. Labeled cells were often noticed to be arranged in clusters, suggesting clonality, and could also be detected within the exposed cartilage of ear wound specimens, morphologically indistinguishable from native chondrocytes (Fig. 4). In that capacity, the aMSCs were possibly recapitulating their chondrogenic differentiation potential, already described in vitro [13,22]. The absence of ovine-validated antibodies to confirm chondrogenic identity in vivo precluded us from furthering this particular analysis beyond purely morphological data, however.

The fact that the labeled cells were found within fresh primary and secondary intention healing wounds (cervical and ear, respectively), as well as midterm (thoracic) wounds suggested a ubiquitous participation of aMSCs in fetal

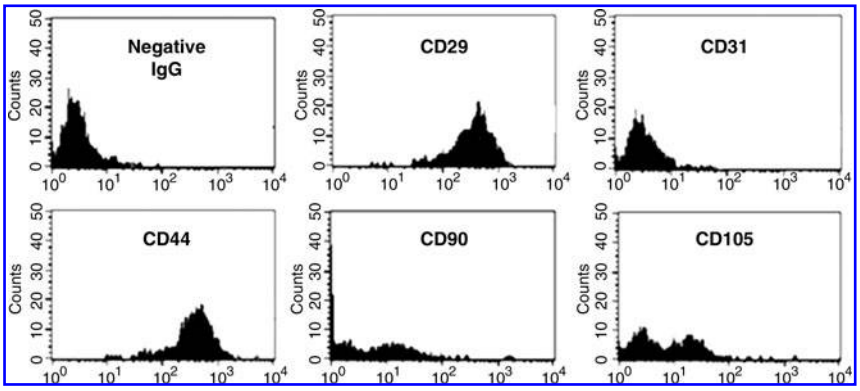

FIG. 2. Representative immunophenotypic analysis of ovine amniotic mesenchymal stem cells by flow cytometry.

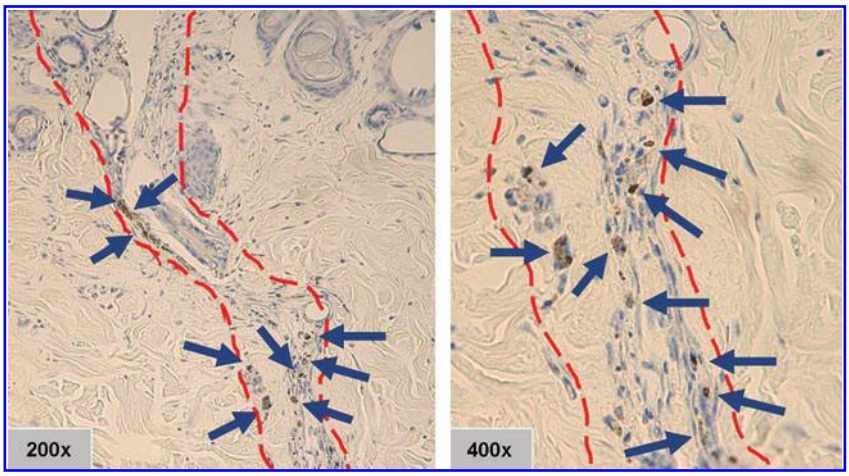

FIG. 3. Transverse views of cervical wounds healing by primary intention (within the *dotted lines*), at different magnifications. Labeled autologous amniotic mesenchymal stem cells can be identified on monoclonal anti-green fluorescent protein immunohistochemistry (*arrows*) selectively populating the wounds. Color images available online at www.liebertonline.com/scd

wound healing, as well as in subsequent wound remodeling. These cells could also incorporate into injured cartilage, apparently differentiating into chondrocytes in vivo.

Experiment II

Overall, selectively covered wounds showed a significantly slower healing rate than control wounds, based on absolute residual open wound area comparisons (group-by-time slope test: $F = 5.57$; $P = 0.005$). At the early time points, namely, POD 5 or 6, the residual open area was not significantly different between covered and control wounds (respectively, 79 vs. 82 mm^2; $P = 0.80$). However, covered wounds remained significantly larger than control wounds at POD 9 (59 vs. 14 mm^2; $P < 0.001$) and POD 20 (31 vs. 3 mm^2; $P = 0.01$; Figs. 5 and 6). By POD 32, all fetal wounds, regardless of group, were fully healed (Fig. 6).

Histologically, time-dependent differences in wound epithelialization were in accordance with the gross observations described above. The minimal inflammation typical of fetal wound healing and positive expression of Substance P on immunohistochemistry were noted in all wounds, with no distinguishable difference between the groups. Masson's trichrome and Van Gieson's stains qualitatively suggested an augmentation of extracellular matrix deposition over time in both wound groups, as did the immunostaining for collagen type-III.

Quantitative extracellular matrix comparisons showed a significant time-dependent increase in elastin and collagen levels in both wound types (both $P < 0.01$; Fig. 7). However, paired comparisons indicated significantly lower elastin levels in covered wounds at the 3 mid time points (POD 9–22 vs. 26 mcg/mg; POD 14–22 vs. 26 mcg/mg; and POD 20–29

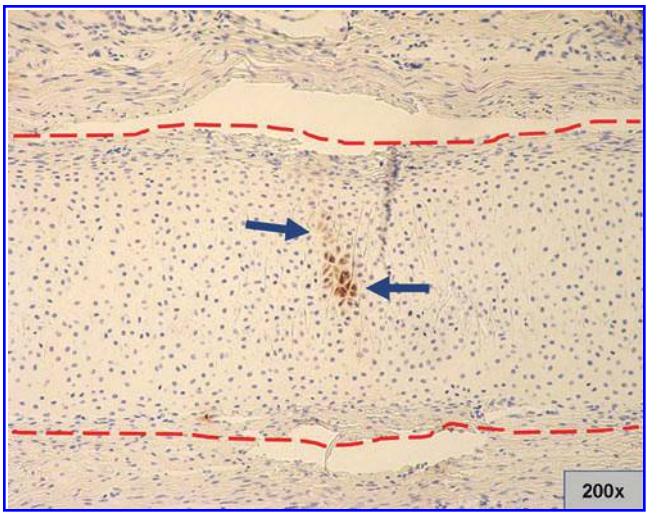

FIG. 4. Cluster of labeled autologous amniotic mesenchymal stem cells identified on monoclonal anti-green fluorescent protein immunohistochemistry (*arrows*) selectively populating the cartilage exposed within open transverse ear wounds, healing by secondary intention. The area in between the *dotted lines* comprises the cartilage exposed through the open ear wound, with the ear's skin and subcutaneous tissue visible beyond these lines. The labeled cells' morphology is indistinguishable from that of adjacent native chondrocytes. Color images available online at www.liebertonline.com/scd

FIG. 5. Representative gross view of 2 sets of open (controls, *on the left*) and covered (*on the right*) fetal wounds, each set from the same animal, on postoperative days 9 **(A)** and 20 **(B)**, illustrating the evident differences in healing rate. Color images available online at www.liebertonline.com/scd

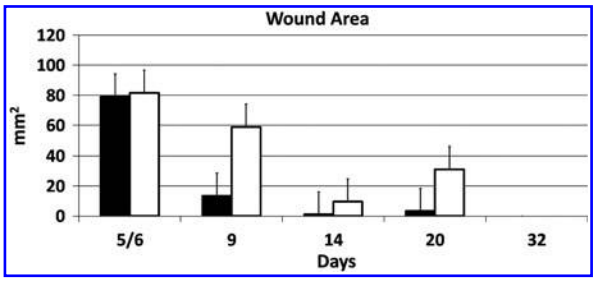

FIG. 6. Quantitative time-dependent changes in residual wound area of open (control) and covered fetal wounds. All wounds were fully healed at 32 days postoperatively. ■ control; □ covered.

vs. 37 mcg/mg; all $P < 0.01$). As to collagen, the only time point at which there was a significant difference was POD 32, when the covered group had significantly lower levels (57 vs. 71 mcg/mg; $P < 0.04$). In both covered and control groups, hyaluronic acid levels were significantly higher at the early time points, lowering at each time point subsequent to POD 9 (POD 14—$P < 0.01$; POD 20—$P = 0.05$; and POD 32—$P < 0.01$). Despite an overall trend toward higher levels in the covered wounds, hyaluronic acid levels were not significantly different between the groups within the power of this study, power being a perennial constraint of large animal models.

Discussion

Taken in combination, the findings from our 2 experiments shed light on an element of fetal wound healing, namely, an ectopic yet autologous cellular component—amniotic cells—which has been entirely overlooked up to now. The rationale behind the sequence of experiments undertaken here stemmed from the need to determine whether the presence of aMSCs in the fetal wounds, as revealed in experiment I, was not simply an epiphenomenon, rather than an active component of the healing process. The results of experiment II point to an active role of amniotic cells in such a process. Although all wounds in experiment II did eventually heal, the pace of the healing process, as well as certain peculiarities of the wound milieu, more specifically its extracellular matrix profile, were negatively impacted by the selective absence of amniotic cells in the closed wounds. The fractal dimensions of the pores that constituted the semipermeable membrane employed to close the wounds in that experiment allows one to link the effects of the wound closure to the lack of amniotic cells, rather than of any local macromolecule. One limitation of our experimental design, however, was the fact that it was not possible, at least by mechanical means such as a semipermeable membrane, to selectively control the local traffic of one or more specific cell types. Hence, we could not rule out the fact that amniotic cells other than aMSCs might also be playing a role in the healing process.

Of course, there is ample evidence that fetal wound healing is a complex process, likely not chiefly governed by an exogenous, even if autologous, cellular component. For example, marsupial fetuses exhibit improved wound repair even after they have left the marsupial pouch. Still, their healing postpouch life is not as enhanced as it is while within the pouch and there is a general temporal correlation between pouch life and transition into a scarring phenotype [23,24]. Yet other evidence is the fact that fetal fibroblasts synthesize more collagen, particularly type-III, and migrate faster than their adult counterparts, both of which are characteristics known to impact wound healing [2,25]. Still, our results underline yet another relevant component of this process that had yet to be recognized.

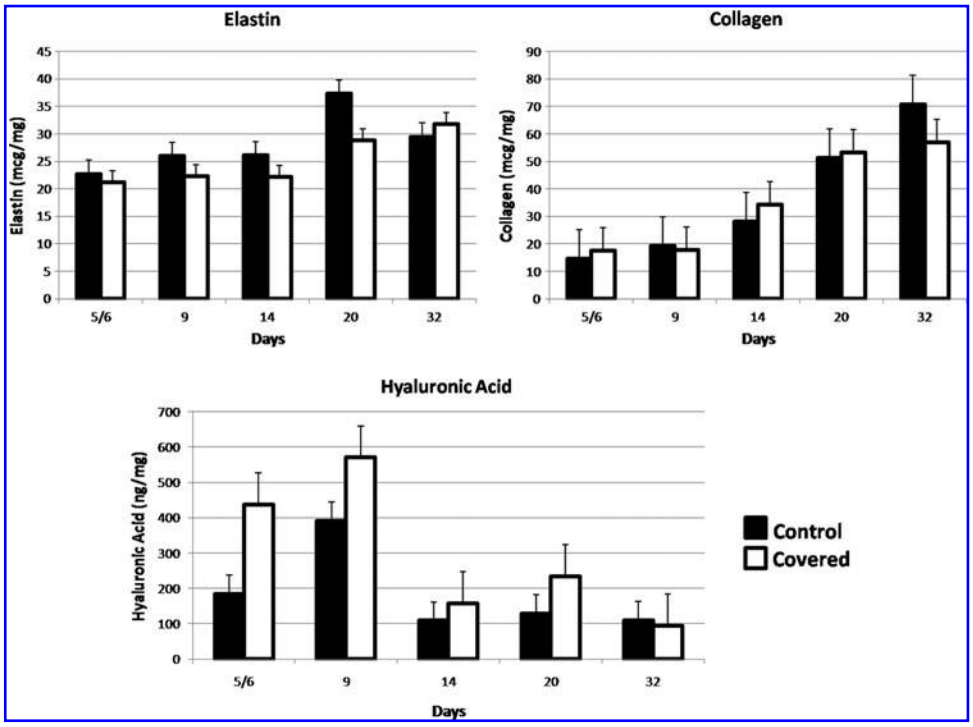

FIG. 7. Quantitative time-dependent changes in different major extracellular matrix components within open (control) and covered fetal wounds.

It was paramount for our experiments to be conducted in a large animal model well suited for the study of fetal biology and surgery, which allowed for >1 prenatal surgical manipulation with enough time for consequential cell processing in between the procedures in experiment I, as well as for time-related analyses in experiment II. On the other hand, a drawback of this model was that it was not conducive to an indepth analysis of the mechanisms behind the phenomena we have observed, due to the notorious unavailability of microarrays for pathway-specific analyses in large/domestic animals, including sheep. From a mechanistic perspective, however, our data at least allow for a few pertinent speculations in light of current general knowledge on wound healing and aMSCs. In experiment I, labeled aMSCs preferentially migrated to the areas of injury. Hyaluronic acid may have been one of the factors acting as a homing or chemotactic signal recognized by the aMSCs. The default pathway of differentiation of aMSCs is the fibroblastic lineage. Previous leporine models have shown that fetal fibroblasts have an increased density of cell surface hyaluronic acid receptors compared with adult counterparts [26]. Elevated hyaluronic acid levels make the fetal wound matrix more welcoming of a fibroblast influx, including possibly phenotypically related cells from the amniotic fluid, such as aMSCs. Indeed, the trend toward higher hyaluronic acid levels observed in the covered wounds may have been at least in part related to the semipermeable membrane restricting the influx of aMSCs to these areas. More recently, Substance P has been shown to be upregulated in postnatal animal models of wound healing and to act systemically as a messenger of injury. The resultant mobilization of CD29+ cells in response to Substance P leads to accelerated wound healing, seemingly by stimulating cell proliferation, activation of the extracellular signal-related kinases 1 and 2, and nuclear translocation of beta-catenin, adding yet another germane element to the wound healing puzzle [27]. We have documented Substance P expression in all fetal wounds and aMSCs are robustly CD29+. Further, a number of other growth factors and cytokines are known to be upregulated during the inflammatory phase of wound healing, including transforming growth factor-β isoforms, interleukin-8, interleukin-6, and tumor necrosis factor-α [28]. These and other factors have been shown to be secreted by aMSCs, at least in certain culture conditions in vitro [29]. Such aMSC-preconditioned media have been used to augment dermal fibroblast migration in vitro and to enhance experimental postnatal wound healing in vivo, implying a role for paracrine factors produced by aMSCs in tissue repair [29]. All these previous data are in line with and add to our findings as to a consequential role of aMSCs in fetal wound healing.

aMSCs proliferate more than twice as quickly in culture than bone marrow- and umbilical cord blood-derived mesenchymal stem cells of indistinguishable phenotype, when grown under identical conditions in vitro [13]. For example, a 3–5 mL aliquot of amniotic fluid obtainable during a routine diagnostic amniocentesis is all that would be needed for one to obtain several hundred million cells in 3–4 weeks' time [30,31]. The mechanisms behind this remarkably enhanced self-renewal capacity of aMSCs have yet to be determined, yet such robust proliferation kinetics may be germane to the biological role hereby unveiled. In like manner, the previously demonstrated unique matrix deposition patterns of aMSCs in vitro when compared with that of other mesenchymal stem cells may also be relevant to their role in fetal repair [13].

The unavoidable constraints of the present experiments notwithstanding, to our knowledge, they provide first evidence of a biological role for any amniotic cell and, in particular, for aMSCs. These observations also add a new dimension to fetal and general wound healing, as well as lend further support to the use of aMSCs in a spectrum of conceivable cell-based regenerative strategies, both perinatally and later in life [10,30–37].

Acknowledgments

S.A.S. was supported by the Joshua Ryan Rappaport Fellowship of the Department of Surgery at Children's Hospital Boston. D.O.F. was supported by a Translational Research Program Award from Children's Hospital Boston. The authors are indebted to Arthur Nedder, D.V.M., and Mr. Mark Kelly for their exemplary veterinary care.

Author Disclosure Statement

No competing financial interests exist.

References

1. Gurtner GC, S Werner, Y Barrandon and MT Longaker. (2008). Wound repair and regeneration. Nature 453:314–321.
2. Tammi R, S Pasonen-Seppanen, E Kolehmainen and M Tammi. (2005). Hyaluronan synthase induction and hyaluronan accumulation in mouse epidermis following skin injury. J Invest Dermatol 124:898–905.
3. David-Raoudi M, F Tranchepain, B Deschrevel, JC Vincent, P Bogdanowicz, K Boumediene and JP Pujol. (2008). Differential effects of hyaluronan and its fragments on fibroblasts: relation to wound healing. Wound Repair Regen 16:274–287.
4. Fauza D. (2004). Amniotic fluid and placental stem cells. Best Pract Res Clin Obstet Gynaecol 18:877–891.
5. Tsai MS, JL Lee, YJ Chang and SM Hwang. (2004). Isolation of human multipotent mesenchymal stem cells from second-trimester amniotic fluid using a novel two-stage culture protocol. Hum Reprod 19:1450–1456.
6. Tsai MS, SM Hwang, YL Tsai, FC Cheng, JL Lee and YJ Chang. (2006). Clonal amniotic fluid-derived stem cells express characteristics of both mesenchymal and neural stem cells. Biol Reprod 74:545–551.
7. Wu Y, J Wang, PG Scott and EE Tredget. (2007). Bone marrow-derived stem cells in wound healing: a review. Wound Repair Regen 15 (Suppl. 1):S18–S26.
8. Kwong FN and MB Harris. (2008). Recent developments in the biology of fracture repair. J Am Acad Orthop Surg 16:619–625.
9. Fu X and H Li. (2009). Mesenchymal stem cells and skin wound repair and regeneration: possibilities and questions. Cell Tissue Res 335:317–321.
10. Kaviani A, TE Perry, A Dzakovic, RW Jennings, MM Ziegler and DO Fauza. (2001). The amniotic fluid as a source of cells for fetal tissue engineering. J Pediatr Surg 36:1662–1665.
11. Perry TE, S Kaushal, FW Sutherland, KJ Guleserian, J Bischoff, M Sacks and JE Mayer. (2003). Thoracic Surgery Directors Association Award. Bone marrow as a cell source for tissue engineering heart valves. Ann Thorac Surg 75:761–767; discussion 767.
12. Krupnick AS, KR Balsara, D Kreisel, M Riha, AE Gelman, MS Estives, KM Amin, BR Rosengard and AW Flake. (2004).

Fetal liver as a source of autologous progenitor cells for perinatal tissue engineering. Tissue Eng 10:723–735.
13. Kunisaki SM, JR Fuchs, SA Steigman and DO Fauza. (2007). A comparative analysis of cartilage engineered from different perinatal mesenchymal progenitor cells. Tissue Eng 13: 2633–2644.
14. Puchtler H and SN Meloan. (1978). Demonstration of phosphates in calcium deposits: a modification of von Kossa's reaction. Histochemistry 56:177–185.
15. Cherry SR, D Biniszkiewicz, L van Parijs, D Baltimore and R Jaenisch. (2000). Retroviral expression in embryonic stem cells and hematopoietic stem cells. Mol Cell Biol 20:7419–7426.
16. Langenau DM, D Traver, AA Ferrando, JL Kutok, JC Aster, JP Kanki, S Lin, E Prochownik, NS Trede, LI Zon and AT Look. (2003). Myc-induced T cell leukemia in transgenic zebrafish. Science 299:887–890.
17. Eriksson E and J Vranckx. (2004). Wet wound healing: from laboratory to patients to gene therapy. Am J Surg 188:36–41.
18. Dougherty G. *Digital Image Processing for Medical Applications*. (2009). Cambridge University Press, Cambridge, United Kingdom.
19. Fuchs JR, S Terada, D Hannouche, ER Ochoa, JP Vacanti and DO Fauza. (2002). Engineered fetal cartilage: structural and functional analysis in vitro. J Pediatr Surg 37:1720–1725.
20. Chockalingam PS, W Zeng, EA Morris and CR Flannery. (2004). Release of hyaluronan and hyaladherins (aggrecan G1 domain and link proteins) from articular cartilage exposed to ADAMTS-4 (aggrecanase 1) or ADAMTS-5 (aggrecanase 2). Arthritis Rheum 50:2839–2848.
21. Sokal RR and FJ Rohlf. (1995). *Biometry: The Principles and Practice of Statistics in Biological Research*. W. H. Freeman, New York.
22. Kunisaki SM, RW Jennings and DO Fauza. (2006). Fetal cartilage engineering from amniotic mesenchymal progenitor cells. Stem Cells Dev 15:245–253.
23. Armstrong JR and MW Ferguson. (1995). Ontogeny of the skin and the transition from scar-free to scarring phenotype during wound healing in the pouch young of a marsupial, *Monodelphis domestica*. Dev Biol 169:242–260.
24. Morykwas MJ, JA Ditesheim, MS Ledbetter, E Crook, WL White, DA Jennings and LC Argenta. (1991). *Monodelphis domesticus*: a model for early developmental wound healing. Ann Plast Surg 27:327–331.
25. Gosiewska A, CF Yi, LJ Brown, B Cullen, D Silcock and JC Geesin. (2001). Differential expression and regulation of extracellular matrix-associated genes in fetal and neonatal fibroblasts. Wound Repair Regen 9:213–222.
26. Alaish SM, D Yager, RF Diegelmann and IK Cohen. (1994). Biology of fetal wound healing: hyaluronate receptor expression in fetal fibroblasts. J Pediatr Surg 29:1040–1043.
27. Hong HS, J Lee, E Lee, YS Kwon, W Ahn, MH Jiang, JC Kim and Y Son. (2009). A new role of substance P as an injury-inducible messenger for mobilization of CD29(+) stromal-like cells. Nat Med 15:425–435.
28. Singer AJ and RA Clark. (1999). Cutaneous wound healing. N Engl J Med 341:738–746.
29. Yoon BS, JH Moon, EK Jun, J Kim, I Maeng, JS Kim, JH Lee, CS Baik, A Kim, KS Cho, HH Lee, KY Whang and S You. (2010). Secretory profiles and wound healing effects of human amniotic fluid-derived mesenchymal stem cells. Stem Cells Dev 19:887–902.
30. Kunisaki SM, M Armant, GS Kao, K Stevenson, H Kim and DO Fauza. (2007). Tissue engineering from human mesenchymal amniocytes: a prelude to clinical trials. J Pediatr Surg 42:974–979; discussion 979–980.
31. Steigman SA, M Armant, L Bayer-Zwirello, GS Kao, L Silberstein, J Ritz and DO Fauza. (2008). Preclinical regulatory validation of a 3-stage amniotic mesenchymal stem cell manufacturing protocol. J Pediatr Surg 43:1164–1169.
32. Kaviani A, K Guleserian, TE Perry, RW Jennings, MM Ziegler and DO Fauza. (2003). Fetal tissue engineering from amniotic fluid. J Am Coll Surg 196:592–597.
33. Fuchs JR, A Kaviani, JT Oh, D LaVan, T Udagawa, RW Jennings, JM Wilson and DO Fauza. (2004). Diaphragmatic reconstruction with autologous tendon engineered from mesenchymal amniocytes. J Pediatr Surg 39:834–838; discussion 834–838.
34. Kunisaki SM, JR Fuchs, A Kaviani, JT Oh, DA LaVan, JP Vacanti, JM Wilson and DO Fauza. (2006). Diaphragmatic repair through fetal tissue engineering: a comparison between mesenchymal amniocyte- and myoblast-based constructs. J Pediatr Surg 41:34–39; discussion 34–39.
35. Kunisaki SM, DA Freedman and DO Fauza. (2006). Fetal tracheal reconstruction with cartilaginous grafts engineered from mesenchymal amniocytes. J Pediatr Surg 41:675–682.
36. Schmidt D, J Achermann, B Odermatt, C Breymann, A Mol, M Genoni, G Zund and SP Hoerstrup. (2007). Prenatally fabricated autologous human living heart valves based on amniotic fluid derived progenitor cells as single cell source. Circulation 116:I64–I70.
37. Steigman SA, A Ahmed, RM Shanti, RS Tuan, C Valim and DO Fauza. (2009). Sternal repair with bone grafts engineered from amniotic mesenchymal stem cells. J Pediatr Surg 44:1120–1126; discussion 1126.

Address correspondence to:
Dr. Dario O. Fauza
Department of Surgery
Children's Hospital Boston and Harvard Medical School
Fegan 3-300 Longwood Avenue
Boston, MA 02115

E-mail: dario.fauza@childrens.harvard.edu

Received for publication September 1, 2010
Accepted after revision October 27, 2010
Prepublished on Liebert Instant Online October 27, 2010